Title

Air quality diagnosis from comprehensive observations of total OH reactivity and reactive trace species in urban central Tokyo

Authors

Yoshino, Ayako
Nakashima, Yoshihiro
Miyazaki, Koji
et al.

Publication Date

2012-03-01

DOI

10.1016/j.atmosenv.2011.12.029

Atmospheric Environment 49 (2012) 51–59

Contents lists available at SciVerse ScienceDirect

Atmospheric Environment

journal homepage: www.elsevier.com/locate/atmosenv

Air quality diagnosis from comprehensive observations of total OH reactivity and reactive trace species in urban central Tokyo

Ayako Yoshino [a,*], Yoshihiro Nakashima [a], Koji Miyazaki [a], Shungo Kato [a], Jeeranut Suthawaree [a], Nobuo Shimo [b], Sou Matsunaga [b], Satoru Chatani [b,c], Eric Apel [d], James Greenberg [d], Alex Guenther [d], Hiroyuki Ueno [e], Hiroyuki Sasaki [e], Jun-ya Hoshi [e], Hisashi Yokota [e], Koichiro Ishii [e], Yoshizumi Kajii [a]

[a] Department of Applied Chemistry, Graduate School of Urban Environmental Sciences, Tokyo Metropolitan University, 1-1 Minami-Osawa, Hachioji, Tokyo 192-0397, Japan
[b] Auto Oil and New Fuels Department, Japan Petroleum Energy Center, 4-3-9 Toranomon, Minato-ku, Tokyo 105-0001, Japan
[c] Toyota Central R&D Laboratories Inc., 41-1 Aza Yokomichi, Oaza Nagakute, Nagakute-cho, Aichi-gun, Aichi 480-1192, Japan
[d] Atmospheric Chemistry Division, National Center for Atmospheric Research, 3450 Mitchell Lane, Boulder, CO 80301, USA
[e] Tokyo Metropolitan Research Institute for Environmental Protection, 1-7-5 Shinsuna, Koto-ku, Tokyo 136-0075, Japan

ARTICLE INFO

Article history:
Received 14 July 2011
Received in revised form
6 December 2011
Accepted 13 December 2011

Keywords:
Urban air quality
Total OH reactivity
Tropospheric ozone
Volatile organic compounds

ABSTRACT

We have conducted a comprehensive observational study to determine the mixing ratios of atmospheric chemical species and total OH reactivity in central Tokyo, in order to diagnose the air quality during summer and winter 2007 and autumn 2009. Concentrations of over 70 reactive trace species were continuously measured throughout each season. The total OH reactivity was measured directly using a laser-induced pump and probe technique. The observed chemical species exhibited seasonal variations. There was a good correlation between NO and CO in winter, but not in summer. This indicates that during winter, vehicle exhaust provided a significant source of NO in central Tokyo, while photolysis of NO_2 was dominant in summer. Similar values (approximately 30 s^{-1}) for the averaged total OH reactivity were observed in both summer and autumn during the daytime. However, VOCs accounted for a larger percentage of the OH reactivity in summer, while NO_x was more dominant in autumn. We find that photochemical processes leading to oxidant production via VOCs dominated OH removal in summer, while the production of nitric acid from the reaction between OH and NO_2 was dominant in autumn, by-passing the oxidant production pathways and resulting in reduced oxidant formation.

1. Introduction

In the past three decades, the increase in tropospheric ozone (O_3) concentration has remained a significant problem in most cities in Japan, even though the levels of ozone precursors such as nitrogen oxides (NO_x) and volatile organic compounds (VOCs) have decreased following the successful implementation of emission controls on vehicle exhaust (Bureau of Environment, Tokyo Metropolitan Government, 2010; Tajima et al., 2010). The concentration of NO_x ($NO_x = NO + NO_2$) and non-methane hydrocarbons (NMHCs) has decreased by 10%–20%, while in contrast, O_3 has increased by 2% per year between 1992 and 2002 in Japan (Akimoto, 2006). Tropospheric O_3 makes a significant contribution to global warming because of its large radiative forcing, which is nearly equal to that of methane (CH_4). Thus there is a need within the atmospheric science community to investigate the cause of this increase in tropospheric O_3. Recent research has suggested that factors responsible for this increase in O_3 may include the presence of unknown VOCs (Sadanaga et al., 2005; Kajii et al., 2006) which facilitate highly efficient O_3 production following the decrease in NO_x, the acceleration of O_3 production by the heat island phenomenon, and the transport of O_3 and its precursors from the Asian continent (Ohara and Sakata, 2003). However, the most significant causative factors of this increase in O_3 in the urban atmosphere have yet to be identified. In order to completely understand the mechanism of tropospheric O_3 production, simultaneous observations of all the precursors of O_3 and an understanding of their reaction pathways are necessary, but this is not a practical approach. A great number of reactions contribute to the formation of tropospheric O_3. Lewis et al. (2000) reported that there are more than several hundred kinds of VOCs in the troposphere, and Goldstein and Galbally (2007) reported that there are probably more than 10^5 different VOCs in the troposphere, which underscores the difficulty in fully characterizing all tropospheric O_3 reaction pathways.

* Corresponding author. Present address: Faculty of Agriculture, Tokyo University of Agriculture and Technology, 3-5-8 Saiwaicho, Fuchu, Tokyo 183-8509, Japan. Tel./fax: +81 42 367 5620.
E-mail address: ayoshino@cc.tuat.ac.jp (A. Yoshino).

1352-2310/$ – see front matter © 2011 Elsevier Ltd. All rights reserved.
doi:10.1016/j.atmosenv.2011.12.029

The measurement of total OH reactivity (k_{OH}), however, provides comprehensive information regarding OH loss processes, which include the reactions of almost all chemical species with OH in the atmosphere. These reactions constitute the first step in the process of photochemical O_3 production in the atmosphere. Total OH reactivity measurements in the urban atmosphere have been conducted in New York City, USA (Ren et al., 2003a, 2003b, 2006), Mexico City, Mexico (Shirley et al., 2006), Mainz, Germany (Sinha et al., 2008), Pearl River Delta, China (Hofzumahaus et al., 2009; Lou et al., 2010), and Houston, USA (Mao et al., 2010). The values of the OH reactivity observed during these measurements vary widely, between 10 and 200 s^{-1}, which reflects considerable regional diversity in the urban atmosphere. Consequently further observations in many different locations together with an improved understanding of photochemical reaction processes in the atmosphere are required. We have previously conducted direct measurements of total OH reactivity using a laser-induced pump and probe technique at a semi-urban site in Tokyo, at Tokyo Metropolitan University (TMU) in 2003–2004 (Sadanaga et al., 2004b; Yoshino et al., 2006). Here the measured OH reactivity was compared with the OH reactivity calculated from the sum of all individual species measured that contribute to the OH reactivity. The calculated OH reactivity and the directly measured OH reactivity would be in agreement if all the chemical species that react with OH in the atmosphere were measured. The results from these studies, however, showed differences between the directly measured and the calculated values, demonstrating the presence of OH reactions with unmeasured chemical species. This phenomenon is known as the "missing OH reactivity". Unmeasured secondary species produced by photochemical oxidation in the atmosphere likely contributed to these processes since the missing OH reactivity was more significant in the summer and spring. We have also considered the potential O_3 production based upon the directly measured and the calculated OH reactivities. The O_3 production potential obtained from the directly measured OH reactivity was significantly higher than that obtained from calculated OH reactivity, particularly under lower NO_x conditions (<20 ppbv) around TMU (Sadanaga et al., 2005; Kajii et al., 2006). These results indicate that unmeasured species, including secondary products caused by photochemical reactions in the atmosphere, made a significant contribution to the O_3 production. In addition, the missing OH reactivity was also observed in OH reactivity measurements of exhaust from gasoline-fueled vehicles, but the values were around 17–18% of the total OH reactivity, which is smaller than the value of approximately 30% that has been reported based on ambient air measurements (Nakashima et al., 2010). This indicates the presence of unknown species that come from primary emissions as well as secondary productions from photochemical reactions in the atmosphere.

In this study, we conducted intensive observations of reactive trace species in the atmosphere of urban central Tokyo, and have diagnosed the air quality using trace species measurements and direct measurements of the total OH reactivity.

2. Observation

2.1. Site description

All observations were conducted at the Tokyo Metropolitan Research Institute for Environmental Protection (TMRIEP, 35.7 °N, 139.8 °E), which is in Toyocho, Koto-ku, in urban central Tokyo. Fig. 1 shows the location of the site. Our observations were conducted over three seasons—summer (August 21–27, 2007), winter (December 20–21, 2007), and autumn (October 27–30, 2009)—with several days of observation in each season. The sample inlets were situated in the windows of laboratories on the fifth and sixth floors of the TMRIEP main building and were set approximately 20 m above the ground (mean sea level). The observation site is surrounded by roads which experience heavy traffic, as well as many factories and buildings, and thus it is directly affected by primary emissions such as anthropogenic VOCs and NO_x. Furthermore, Tokyo Bay is located approximately 2 km south of the site; hence, the site is also influenced by VOCs from the ocean and SO_2 from ship emissions. The composition of the atmosphere at the site is considered very complex and provides a medium for many chemical reactions. We therefore consider this location representative of urban central areas in Japan.

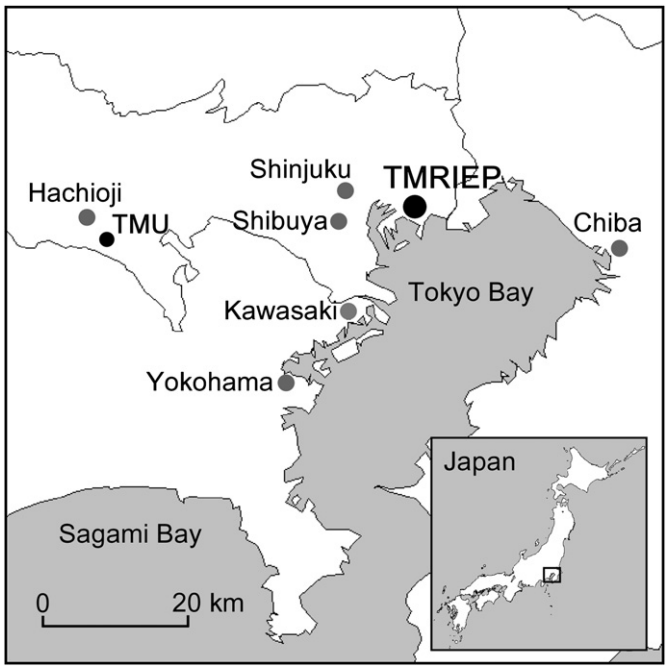

Fig. 1. Location of the observation site at Tokyo Metropolitan Research Institute for Environmental Protection in Toyocho, Koto-ku, Tokyo, in Japan.

2.2. Details of measurements of chemical species in the atmosphere

Trace gas concentrations and the total OH reactivity were measured using the following techniques during each observation period. Meteorological data were also measured.

2.2.1. Measurement of NO_x, CO, O_3, and SO_2

NO_x, CO, O_3, and SO_2 were continuously measured using automated equipment 24 h a day during the observation periods. O_3 was measured by UV absorption (Model 1150, Dylec), CO by non-dispersive infrared spectroscopy (Model 48C, Thermo Electron), and SO_2 by pulsed fluorescence (Model 43CTL, Thermo Electron). NO was measured by O_3 chemiluminescence (Model 42i-TL, Thermo Electron). NO_2 was measured by a laser-induced fluorescence (LIF) technique (Matsumoto et al., 2001; Matsumoto and Kajii, 2003). Sample air was introduced into each instrument through PTFE tubes with a 6.35 mm outside diameter. These measurements were conducted at 1-min averaging intervals. Zero air was introduced into all instruments every hour to measure the zero level of the instrument. The zero air was generated by a zero air generator (Model 111, Thermo Electron), in which chemicals were removed by purafil and charcoal filters and a heated Pt catalyst.

2.2.2. Measurement of VOCs

NMHCs were measured using two instruments. C_2–C_5 NMHCs were measured in situ approximately every half hour during the summer observation period. Samples were analyzed using a gas chromatograph with a flame ionization detector (GC–FID, HP 5890, Hewlett Packard). NMHCs were separated on PLOT (Al_2O_3) capillary columns in a system previously described (Goldan et al., 2000). Concentrations were calibrated with a reference standard (#1660a, 1 ppm propane, National Institute of Standards and Technology, USA). Sample volumes were 250 standard milliliters. Approximately 60 species of C_2–C_{10} NMHCs were also measured using a GC–FID (HP 6890, Hewlett Packard) during all periods. Details of this system were previously described by Kato et al. (2001). The ambient air samples for NMHCs analysis were introduced into stainless steel canisters (3 or 6 L) at 1-h intervals in the daytime. 0.5 L of the sample air was introduced into a three-stage preconcentrator (Model 7000, Entech) to concentrate volatile components prior to injection into the GC–FID and separation using an HP-1 Column (60 m length, 0.32 mm i.d., 1-μm film thickness, Agilent J&W). The temperature of the GC oven was initially kept at −50 °C (for 8 min) and then increased to 40 °C at 5 °C min^{-1}, and subsequently further raised to 150 °C at 15 °C min^{-1}. NMHC concentrations were calibrated with standard gas (Matheson, Enviro-MAT). Detection limits of the NMHCs measured from the canisters by GC–FID are in the range of 1–3 pptv with accuracy of 2–13% and precision of 2–15%. Benzene, toluene, isoprene, and terpenes were measured by means of proton transfer reaction mass spectrometry (PTR/MS) at 1-min averaging intervals to increase the time resolution for the measurement of NMHCs (Kato et al., 2004). Formaldehyde was measured by the Hantzsch reaction using a fluorometric detector (AL4021, AERO-LASER) at 1-min averaging intervals. Oxygenated volatile organic compounds (OVOCs) other than formaldehyde, such as acetaldehyde, acetone, and methanol, were also measured by PTR/MS at 1-min averaging intervals. PTFE tubes with a 6.35 mm o.d. were used for the sample inlets. The zero level of the PTR/MS was also measured every hour using zero air.

2.2.3. Measurement of OH reactivity

OH reactivity was measured every few minutes in the daytime using a laser-induced pump and probe technique (Sadanaga et al., 2004a). Sample air was introduced through a 12.7 mm o.d. PTFE tube into a reaction tube by a diaphragm pump (DA-60S, ULVAC). The flow rate of the sample air was set to 20 SLM using a mass flow sensor (Model 3810S, Kofloc) and needle valve, and the pressure in the reaction tube was maintained at atmospheric pressure. A pulsed 266-nm laser beam from the fourth harmonic of a Nd:YAG laser (Quanta-Ray INDI-40, Spectra physics, or Tempest 300, New Wave Research) was used to irradiate the reaction tube, where it generated OH radicals artificially through the photolysis of O_3 and the reaction with water vapor in the sample air, as follows:

$$O_3 + h\nu(266\ \text{nm}) \rightarrow O_2 + O(^1D) \quad \text{(R1)}$$

$$O(^1D) + H_2O \rightarrow 2OH. \quad \text{(R2)}$$

The repetition rate and the laser energy of the laser beam were set to 2 Hz and around 10 mJ, respectively. The generated OH radicals reacted with the trace species in the sample air, resulting in a decrease in the radical concentration. The changes in the OH concentrations were detected in a fluorescence detection cell by a laser-induced fluorescence technique. A portion of the sample air in the reaction tube was introduced into an LIF cell using a rotary pump (D-950K, ULVAC), and the pressure was maintained at around 2 Torr. An $A^2\Sigma^+ - X^2\Pi(0,0)\ Q_1(2)$ rotation line of OH in the sample air was excited by a second harmonic pulsed dye laser (Scanmate, Lambda Physik, or Precision Scan, Sirah) pumped by a second harmonic pulsed Nd:YVO_4 laser (YHP-40-532Q, Spectra Physics) into the cell to detect the fluorescence of OH. The repetition rate of the laser was set to 10 kHz, and the power was approximately 2–3 mW. The fluorescence signal was detected by a photomultiplier tube (R2256P, Hamamatsu) equipped with a dynode gating system, and the signal was recorded using a photon counting method.

In the autumn period, the sample air was diluted with zero air to remove the influence of OH recycling via the reaction of NO with HO_2 which takes place under high NO conditions. Before and after the OH reactivity measurement, zero air was introduced into the reaction tube and its decay rate was measured each day. The zero air decay rate was measured 8 times each day, and the averaged value of these measurements was applied.

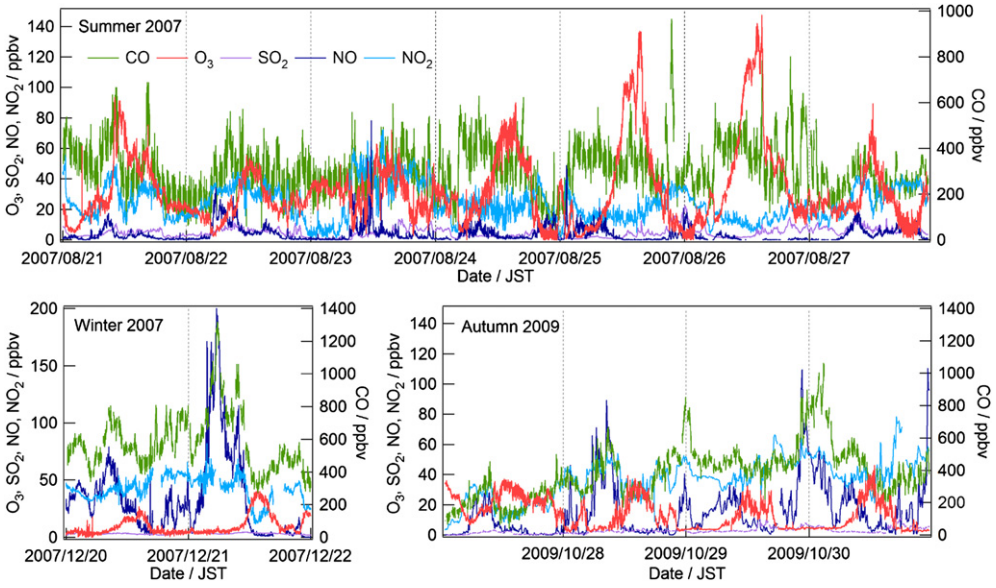

Fig. 2. Diurnal profiles of concentrations of CO, O_3, SO_2, NO and NO_2 for all observations.

3. Results and discussion

3.1. Diurnal profiles of NO_x, CO, O_3, and SO_2

Fig. 2 shows the diurnal variations in the NO_x ($NO_x = NO + NO_2$), CO, O_3, and SO_2 concentrations during all study periods. The averaged daytime concentrations of each species from all observation periods are summarized in Table 1.

O_3 usually exhibits a high concentration during the daytime and a low concentration in the early morning and evening. In this study, O_3 had a daytime peak at around 14:00 and decreased to near zero at night, since the O_3 reaction converting NO to NO_2 results in regeneration of O_3 following NO_2 photolysis during the day, while this pathway does not occur at night. This is a typical diurnal variation regularly observed in the urban atmosphere. The highest mixing ratios of O_3 were above 120 ppbv, on August 25–26 in the summer observation period, during which time there was strong solar radiation. In the winter and autumn, there was a reduced amount of sunlight and the maximum concentrations of O_3 were in the range of 20–40 ppbv.

NO and NO_2 also showed typical diurnal variations for an urban area. The NO concentration was almost zero during the nighttime and increased rapidly in early morning. It then decreased around noon, and increased again in the evening rush hour. This diurnal variation is representative of conditions where vehicle exhaust is the main emission source. NO_2 never decreased to a zero value during the nighttime. In the summer, NO_2 essentially showed a similar variation to NO, but at a consistently higher concentration than NO. However, in the winter, NO_2 showed different behavior to NO, with a relatively constant concentration of around 50 ppbv Fig. 3 shows scatter plots for CO and NO in all seasons. There were good correlations between NO and CO in winter and autumn, but not in the summer. In summer and autumn, the plot shows shallower slopes between CO and NO in the daytime compared to nighttime, with no significant difference found in winter. The good correlations between NO and CO in winter and during nighttime in the autumn reflect air dominated by fresh emissions from vehicle exhaust. In contrast, in summer and the autumn daytime, photolysis of NO_2 provided a significant source of NO in addition to automobile emission sources. The $\Delta CO/\Delta NO$ emission ratio in all seasons was approximately 3–5, as can be seen in Fig. 3. These values were much lower than the emission ratios of 10–150 obtained from the direct measurement of gasoline-fueled vehicles that were compiled with the 2005 Japanese emission control standard (Nakashima et al., 2010). These high emissions of NO were therefore presumably produced by diesel-fueled vehicles and/or gasoline-fueled vehicles that did not comply with the new regulations.

The CO mixing ratio ranged from 200 to 500 ppbv in summer; in winter and autumn, the range of CO values was approximately 500–600 ppbv and often exceeded 1 ppmv. Our measurements suggest that the combustion of fossil fuel contributed significantly as an emission source of CO, since similar trends between CO and NO_2 were observed.

SO_2 was observed at mixing ratios of several ppbv, sometimes exceeding 10 ppbv in summer and autumn. A high level of SO_2 was observed when the wind was from the south, as shown in Fig. 4. Ship emissions from Tokyo Bay would also contribute to the high level of SO_2. In winter, no large fluctuation in SO_2 concentration was observed, and the range was 2–5 ppbv. The source of SO_2 in winter remains unexplained, as there was no correlation between SO_2 and CO.

3.2. Diurnal profiles of VOCs

Fig. 5 shows the diurnal variations of NMHCs in all observation periods. Note that canister samples for NMHCs were not collected

Table 1
Averaged concentrations and standard deviations of observed trace species in daytime from 9:00 to 18:00 during the all periods. Units are all in ppbv.

Chemicals	Summer 2007	Winter 2007	Autumn 2009
CO	329 ± 100	570 ± 172	344 ± 124
O_3	42.8 ± 22.8	14.3 ± 9.91	18.1 ± 9.47
SO_2	5.29 ± 2.67	3.31 ± 0.53	2.88 ± 2.14
NO	5.39 ± 6.31	37.4 ± 33.4	13.8 ± 14.3
NO_2	29.8 ± 12.2	35.8 ± 13.9	43.0 ± 15.9
Alkanes			
Ethane	2.23 ± 1.23	7.54 ± 3.50	3.56 ± 1.23
Propane	2.97 ± 1.77	8.60 ± 4.33	3.61 ± 1.88
Isobutane	2.63 ± 1.87	3.55 ± 1.64	1.95 ± 1.14
n-Butane	4.69 ± 3.65	5.42 ± 2.58	3.08 ± 1.67
Isopentane	4.21 ± 3.25	2.87 ± 1.07	2.04 ± 1.74
n-Pentane	2.14 ± 1.85	1.80 ± 0.91	0.95 ± 0.77
2,2-Dimethylbutane	0.14 ± 0.11	0.43 ± 1.09	0.05 ± 0.04
Cyclopentane	0.19 ± 0.13	0.15 ± 0.07	0.12 ± 0.11
2,3-Dimethylbutane	0.18 ± 0.13	0.41 ± 0.39	0.15 ± 0.13
2-Methylpentane	0.85 ± 0.50	0.92 ± 0.38	0.75 ± 0.64
3-Methylpentane	0.52 ± 0.33	0.64 ± 0.48	0.57 ± 0.57
n-Hexane	1.28 ± 0.74	0.97 ± 0.49	1.40 ± 1.31
Methylcyclopentane	0.31 ± 0.19	0.34 ± 0.17	0.33 ± 0.34
2,4-Dimethylpentane	0.05 ± 0.03	0.04 ± 0.02	0.03 ± 0.04
Cyclohexane	0.39 ± 0.26	0.67 ± 0.51	0.44 ± 0.31
2-Methylhexane	0.15 ± 0.07	0.23 ± 0.12	0.17 ± 0.23
2,3-Dimethylpentane	0.04 ± 0.02	0.07 ± 0.04	0.05 ± 0.05
3-Methylhexane	0.14 ± 0.07	0.24 ± 0.14	0.19 ± 0.22
2,2,4-Trimethylpentane	0.04 ± 0.02	0.05 ± 0.03	0.04 ± 0.03
n-Heptane	0.18 ± 0.09	0.30 ± 0.17	0.20 ± 0.15
Methylcyclohexane	0.13 ± 0.07	0.42 ± 0.23	0.20 ± 0.16
2,3,4-Trimethylpentane	0.02 ± 0.03	0.03 ± 0.02	0.02 ± 0.01
2-Methylheptane	0.03 ± 0.02	0.07 ± 0.04	0.04 ± 0.04
3-Methylheptane	0.03 ± 0.02	0.09 ± 0.04	0.06 ± 0.06
n-Octane	0.19 ± 0.13	0.21 ± 0.12	0.11 ± 0.20
n-Nonane	0.18 ± 0.24	0.43 ± 0.23	0.15 ± 0.09
Alkenes			
Ethylene	2.63 ± 1.47	4.97 ± 2.43	4.36 ± 4.20
Propylene	1.91 ± 1.23	0.96 ± 0.54	1.14 ± 2.56
1-Butene	0.78 ± 3.95	0.24 ± 0.15	0.17 ± 0.27
Butadiene	0.07 ± 0.08	0.09 ± 0.07	0.07 ± 0.07
Trans-2-Butene	0.22 ± 0.42	0.21 ± 0.17	0.11 ± 0.10
Cis-2-Butene	0.22 ± 0.46	0.16 ± 0.12	0.08 ± 0.08
3-Methyl-1-butene	0.06 ± 0.05	0.05 ± 0.02	0.03 ± 0.03
1-Pentene	0.14 ± 0.12	0.16 ± 0.10	0.06 ± 0.07
Trans-2-pentene	0.12 ± 0.09	0.09 ± 0.09	0.08 ± 0.10
Cis-2-pentene	0.05 ± 0.04	0.05 ± 0.04	0.04 ± 0.06
2-Methyl-2-butene	0.13 ± 0.11	0.31 ± 0.22	0.00 ± 0.01
Cyclopentene	0.01 ± 0.01	0.01 ± 0.01	0.02 ± 0.03
4-Methyl-1-pentene	0.07 ± 0.03	0.03 ± 0.04	0.02 ± 0.02
2-Methyl-1-pentene	0.00 ± 0.00	0.01 ± 0.01	0.02 ± 0.03
Trans-2-Hexene	0.02 ± 0.01	0.01 ± 0.01	0.01 ± 0.02
Cis-2-Hexene	0.01 ± 0.01	0.00 ± 0.00	0.01 ± 0.01
Alkyne			
Acetylene	1.41 ± 0.73	3.84 ± 1.59	2.82 ± 3.16
Aromatics			
Benzene	0.78 ± 0.61	0.82 ± 0.28	0.64 ± 0.50
Toluene	2.14 ± 0.99	10.1 ± 5.23	4.79 ± 3.21
Ethylbenzene	0.99 ± 1.52	1.51 ± 0.57	0.90 ± 0.69
p,m-Xylene	1.25 ± 1.72	0.32 ± 0.62	0.79 ± 0.59
Stylene	0.04 ± 0.03	0.14 ± 0.07	0.06 ± 0.04
o-Xylene	0.37 ± 0.38	0.47 ± 0.21	0.31 ± 0.20
Isopropylbenzene	0.03 ± 0.05	0.04 ± 0.02	0.17 ± 0.38
n-Propylbenzene	0.06 ± 0.04	0.13 ± 0.07	0.06 ± 0.05
1,3,5-Trimethylbenzene	0.05 ± 0.05	0.13 ± 0.09	0.08 ± 0.06
1,2,4-Trimethylbenzene	0.22 ± 0.18	0.62 ± 0.36	0.30 ± 0.25
Biogenics			
Isoprene	0.59 ± 0.39	0.06 ± 0.05	0.06 ± 0.04
α-Pinene	0.19 ± 0.25	0.06 ± 0.04	0.11 ± 0.07
β-Pinene	0.03 ± 0.04	0.00 ± 0.00	0.00 ± 0.00
Limonene	0.00 ± 0.00	0.01 ± 0.01	0.02 ± 0.04
Camphene	0.00 ± 0.00	0.00 ± 0.00	0.00 ± 0.01
Oxygenated			
Methanol	36.5 ± 18.9	12.4 ± 4.72	9.03 ± 9.79
Formaldehyde	6.26 ± 2.70	6.48 ± 1.56	3.37 ± 2.04
Acetaldehyde	4.79 ± 2.95	1.56 ± 0.67	1.21 ± 0.84
Acetone	19.7 ± 8.18	2.76 ± 1.12	2.19 ± 0.19

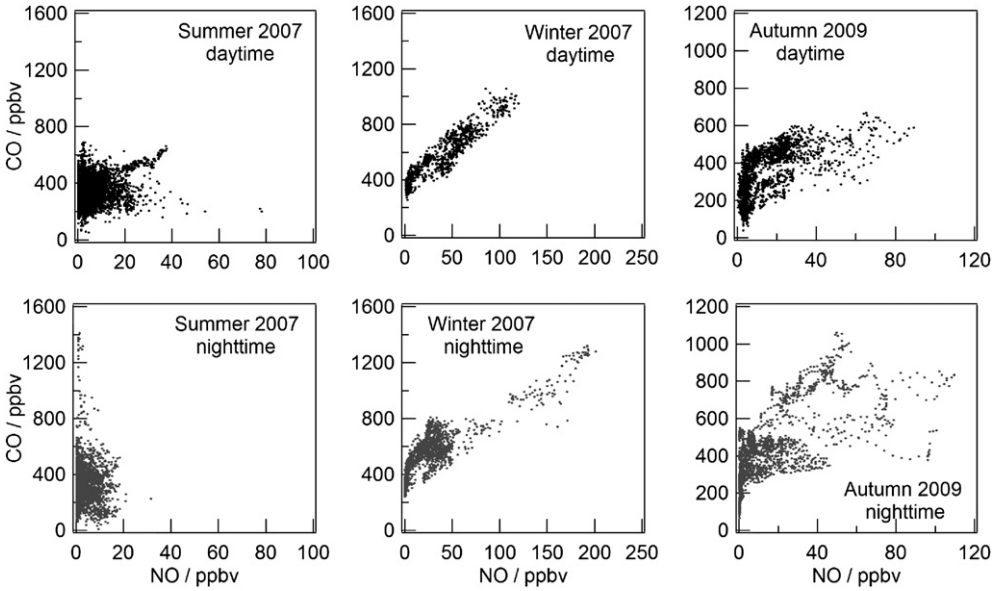

Fig. 3. Scatter plots of CO and NO for all observations. Upper tiles represent daytime and lower tiles represent nighttime for each season.

on August 24 and 25, 2007. The averaged daytime concentrations of each species for different seasons are summarized in Table 1. The averaged concentrations of anthropogenic NMHCs such as alkanes, alkenes, and alkynes decreased in order of increasing carbon number in all seasons, because reactivity with OH and/or O_3 and boiling point increase with increasing molecular weight. Our findings are similar to those from previous observations in Hachioji, a suburban area of Tokyo (Tajima et al., 2010). Alkanes accounted for approximately 60% of the total NMHCs in all observations, alkenes 20%, aromatics 10%, and biogenics 2%. Most NMHCs (e.g., ethane, propane, ethylene, and toluene) showed higher mixing ratios in winter than in summer, with autumn mixing ratios in between the winter and summer seasonal averages. Ethane, propane, and ethylene all have a comparatively low reactivity with OH, and their loss processes by OH were limited in winter because of the diminished photoproduction of OH. In summer, isopentane, *n*-pentane, and isoprene concentrations were higher than in winter. Isoprene is emitted from vegetation, especially broad-leaved plants, and thus its emissions increase in summer as a result of higher biological activity. Isoprene is also emitted from automobiles (Sharma et al., 2000; Nakashima et al., 2010) but the much higher concentrations observed in summer at this site

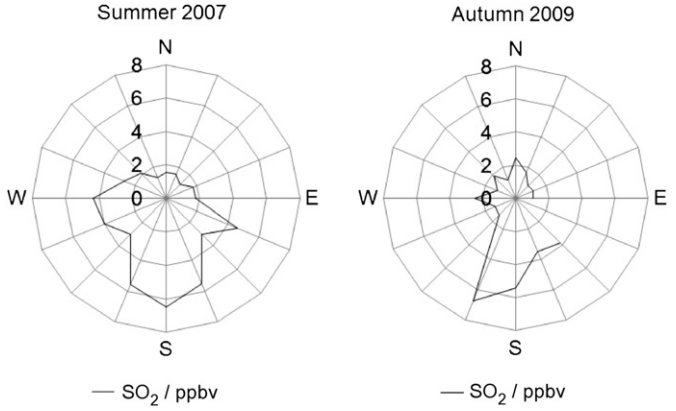

Fig. 4. Averaged concentration of SO_2 for summer and autumn obtained for different wind directions.

demonstrated that biogenic sources of isoprene were dominant. Isopentane and *n*-pentane are emitted from the volatilization of gasoline with increasing atmospheric temperature. Species with short atmospheric lifetimes did not show obvious seasonal variations. Aromatics, including benzene and toluene, showed higher values in winter than in autumn and summer, though the reason for this remains unexplained. The source of these species could be vehicle exhaust, since they showed significant diurnal variation that increased in the morning and evening, and decreased at noon.

Fig. 6 shows the diurnal variation in OVOCs such as methanol, formaldehyde, acetaldehyde, and acetone during all periods. In contrast to NMHCs, most OVOCs showed larger values in summer than in winter and autumn. The formaldehyde, acetaldehyde, and acetone levels in winter and autumn increased in the morning, decreased at noon, and then increased again in the evening. The morning and the evening increments in concentration were due to vehicle exhaust emissions. In summer, these species showed variations similar to those in winter and autumn during the morning, but maintained a relatively large value from noon to evening. This indicates the presence of additional sources of formaldehyde, acetaldehyde, and acetone, and photochemical production processes in the atmosphere which contributed to the increased concentrations from noon to evening. Regarding methanol, the averaged summer concentration was several times larger than the winter value. It should be noted that the elevated concentrations on the evenings of August 22 and 25 were partially due to a strong local source within the laboratory (as a result of changing the dye solution in the laser).

3.3. Diurnal profiles of total OH reactivity

Fig. 7 shows a time series of the observed and calculated OH reactivity for all periods. OH reactivity was not measured on August 24 and 25, 2007. OH reactivity was predicted based upon the observed concentrations of trace gas species and their rate coefficients of reaction with OH (Atkinson, 1994, 1997, 2003, Atkinson et al., 1997; Calvert et al., 2000; Sander et al., 2002). The rate coefficient k_{NO_2} of the OH + NO_2 reaction was obtained from direct measurement in the reaction tube because k_{NO_2} is humidity and pressure dependent (Sadanaga et al., 2004b, 2006). The calculated

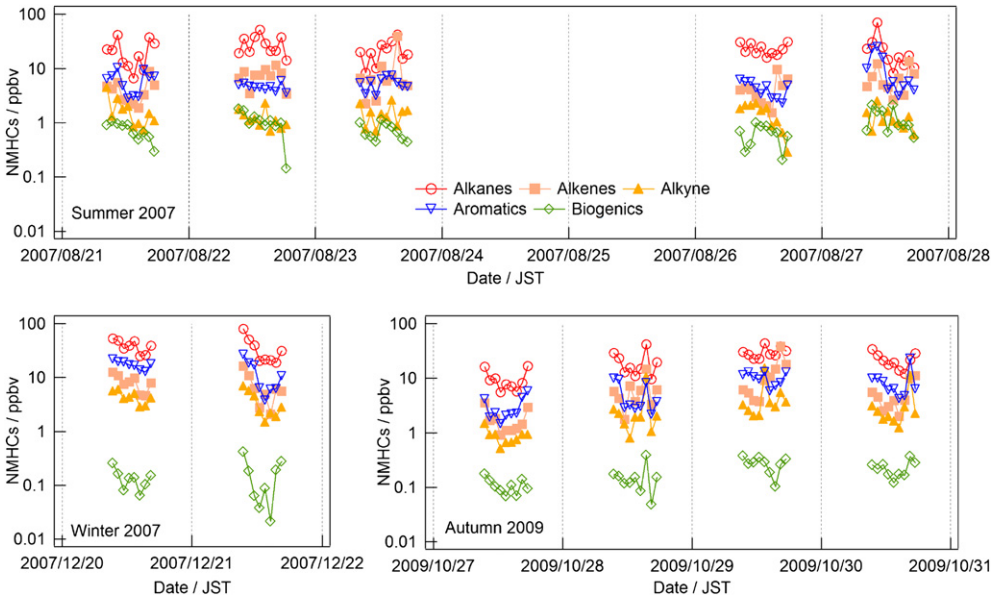

Fig. 5. Diurnal profiles of concentrations of NMHCs from GC–FID analysis for all observations. The NMHC measurements were conducted only in the daytime.

OH reactivity, $k_{OH,}$ is defined as the sum of the products of the observed concentrations and rate coefficients for each species, according to the following formula:

$$k_{OH} = k_{CO}[CO] + k_{O_3}[O_3] + k_{SO_2}[SO_2] + k_{NO_2}[NO_2] + \Sigma k_i[VOCs_i]. \quad (1)$$

The calculated and observed values for OH reactivity were compared. The observed OH reactivity showed a strong fluctuation because trace species change rapidly in an urban atmosphere; this was quite a different result from the observations made in Hachioji, which is 30 km west of Shinjuku, central Tokyo (Yoshino et al., 2006). The observed and calculated values showed a similar variation, which supports this method of measurement of total OH reactivity. In addition, the differences between the observed and the calculated OH reactivity—the missing OH reactivity—were similar to the observations in Hachioji, which indicates the presence of unknown reaction processes of OH radicals. The missing OH reactivity did not show diurnal variations.

In summer, the OH reactivity fluctuated substantially, between 15 and 70 s^{-1}. On August 26, however, the OH reactivity was quite low, in the range 15–30 s^{-1}, because that was a weekend and the air was relatively clean. Differences between the observed and calculated OH reactivity were observed on all days during the summer measurement period. We have previously performed a three-dimensional air quality study which consists of the Weather Research and Forecasting (WRF) model for meteorology, the Community Multi-scale Air Quality (CMAQ) modeling system for pollutant concentrations, and emission inventory models. The model study of OH reactivity in the summer period suggested that unknown secondary products and unidentified primary emitted species contribute to the missing OH reactivity (Chatani et al., 2009). In winter, the observed OH reactivity was in the range of 10–80 s^{-1} and contained large uncertainties. The large

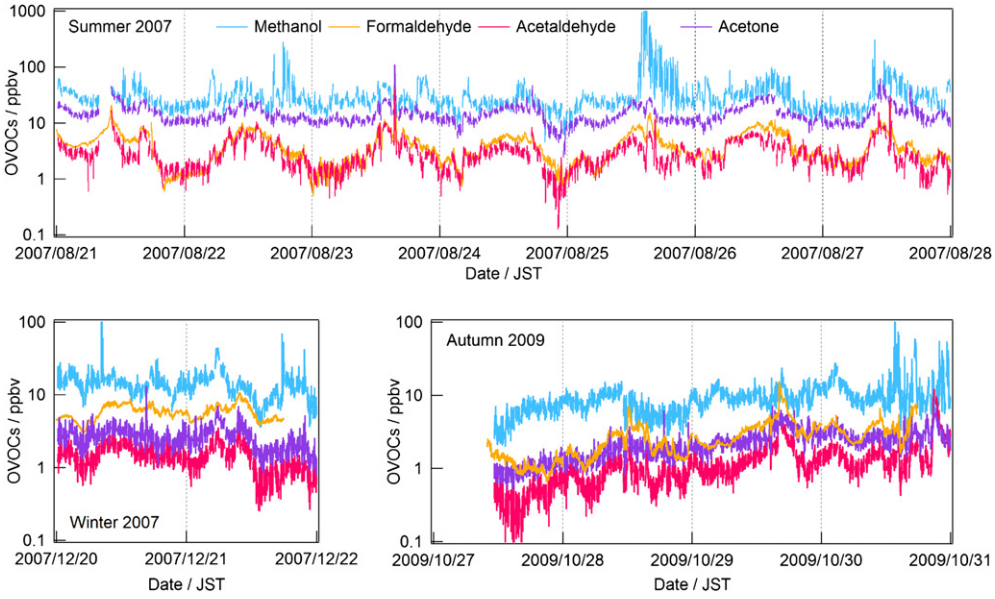

Fig. 6. Diurnal profiles of concentrations of OVOCs from PTR/MS analysis for all observations.

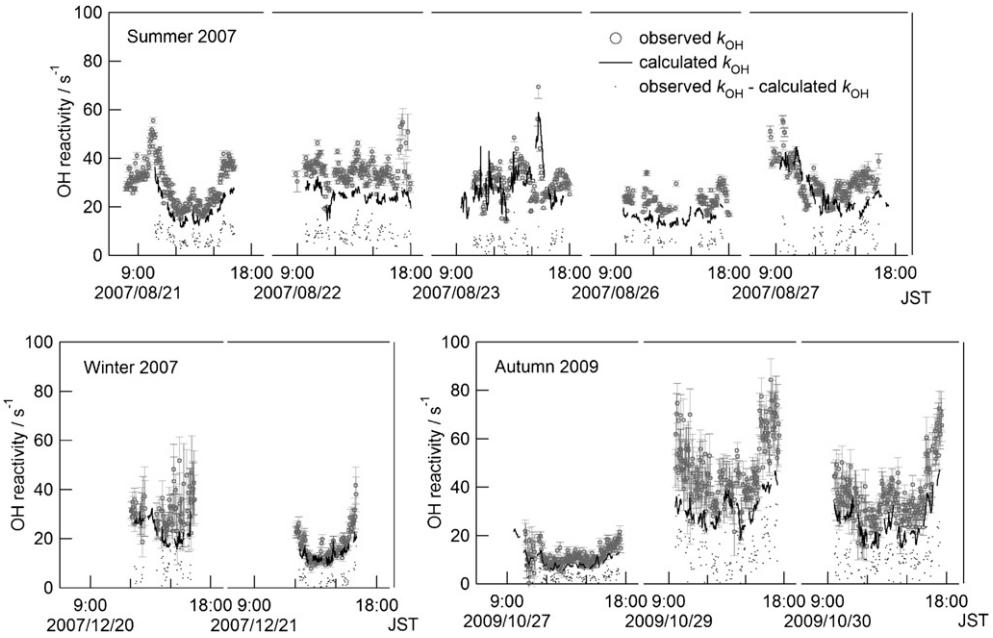

Fig. 7. Time series of observed (open circles) and calculated (lines) total OH reactivity, and their differences (dots) for all observations.

uncertainties in OH reactivity were particularly prominent in the morning, and there were different variations in the observed and the calculated values. This is believed to be due to the OH recycling from the HO_2 + NO reaction, which causes an underestimation of OH reactivity when the NO level is high during the morning rush hour (Sadanaga et al., 2004a; Yoshino et al., 2006). We have excluded these data with large uncertainties from Fig. 7 and later discussions. In autumn, the sample air with high NO_x was diluted to inhibit OH recycling, although the air was not diluted on October 28, thus no data is available for that day. The observed OH reactivity in autumn was in the range 10–80 s^{-1}, relatively similar to winter values. On October 27, which was a very clear and comparatively clean day, the OH reactivity ranged from 10 to 20 s^{-1}. On October 29 and 30, OH reactivity ranged from 30 to 80 s^{-1}, with the values increasing in the morning, decreasing around noon, and increasing again in the evening. The high values in the morning and evening reflect the primary emissions from vehicle exhaust, NO and NO_2 in particular. The inconsistency between the observed and the calculated OH reactivity was small on October 27, a bright, clear day, while it was relatively large on October 29 and 30, which were highly polluted days. During the observations in suburban TMU, the secondary products of atmospheric photochemical reactions contributed to the unknown OH loss processes. However, despite a clear day on October 27, the missing OH reactivity was smaller compared the other days in the autumn observations. The comparatively larger missing OH reactivity observed during autumn compared to summer, especially during the polluted days, suggests that the missing sink in autumn is most likely owing to unmeasured primary emitted species.

3.4. Contribution of each species to total OH reactivity

Fig. 8 shows the percentage contribution of each trace species to the total OH reactivity in all summer and autumn periods. In the figure, the entire 360° circle indicates the observed OH reactivity, and the ratios of each species indicate the calculated OH reactivity of each species. In summer, NO and NO_2 accounted for a quarter of all OH reactivity, at 26.0%. Anthropogenic NMHCs accounted for 22.1%, and OVOCs for 12.4%. Biogenic NMHCs accounted for 5.82% despite their concentration ratio of only 2% of the total VOCs, due to the high reactivity of terpenoid compounds with OH. The total ratios of VOCs accounted for the largest percentage, which exceeded 40% of the total OH reactivity. In autumn, the percentage of NO_2 was the highest, at 31.1%, which combined with NO at 6.19% to account for 37.3% of the total OH reactivity. Anthropogenic NMHCs accounted for 18.0%, OVOCs for 4.88%, and biogenic NMHCs for 0.92%. The total contribution of VOCs was 23.8%. The averaged values of the observed OH reactivity were similar, at 33.4 s^{-1} for the summer period, and 32.3 s^{-1} for the autumn period. VOCs, however, accounted for the highest percentage in summer; in contrast, NO_x made the highest contribution in autumn. These results indicate that the processes of photochemical production of oxidants from VOC and OH reactions are dominant in summer, while the process of nitric acid production from the NO_2 reaction with OH is dominant in autumn.

3.5. Contribution of the missing OH reactivity to photochemical ozone production

If the missing OH reactivity originated from unknown VOCs, the photochemical production of oxidants would be expected to increase with increasing OH reactivity. The ozone production

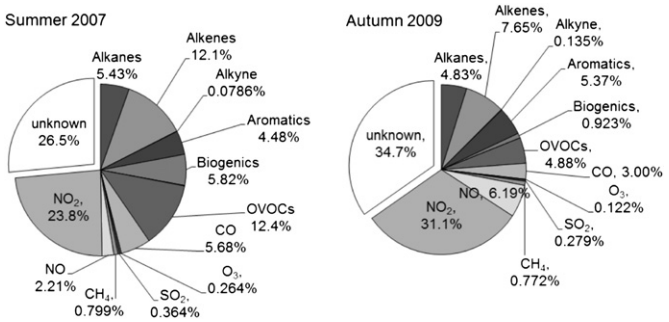

Fig. 8. Contribution of different trace species to total OH reactivity for summer and autumn observations in the daytime (9:00–18:00). Averaged total OH reactivity for each observation period was 33.4 s^{-1} in summer and 32.3 s^{-1} in autumn.

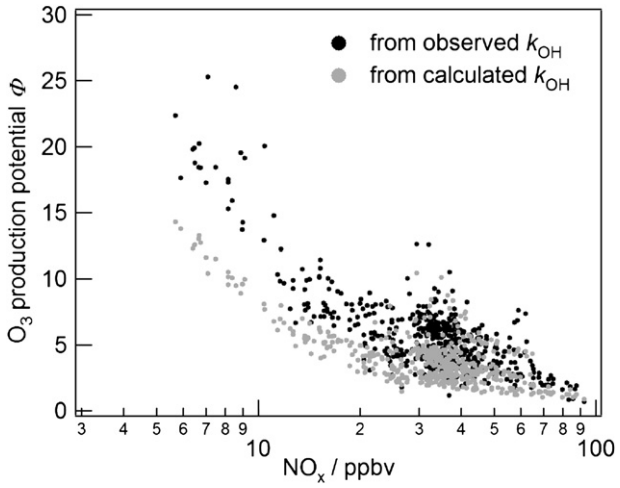

Fig. 9. Ozone production potentials (Φ) with OH reactivity versus concentration of NO_x in the daytime during the summer period. Φ corresponds to the number of accumulated HO_2 and RO_2 radicals through the radical propagation cycle from a single OH radical. The ozone production potentials obtained for observed and calculated OH reactivity are shown as annotated.

potential may be used to investigate the impact of unknown species on production of O_3 and can be calculated using a simple box model. The ozone production potential is defined as the total of HO_2 and RO_2 radicals via reaction of VOC and CO with OH while the concentration of OH is controlled by the reaction between OH and NO_2. Detailed descriptions of the model can be found in Sadanaga et al. (2005). The chain reactions involved are as follows.

$$OH + VOC_i \rightarrow R_iO_2 \quad : k_{1i} \tag{R3}$$

$$OH + CO \rightarrow HO_2 \quad : k_2 \tag{R4}$$

$$OH + NO_2 \rightarrow HNO_3 \quad : k_3 \tag{R5}$$

$$RO_2 + NO + O_2 \rightarrow NO_2 + HO_2 + \text{carbonyls} \quad : k_4 \tag{R6}$$

$$HO_2 + NO \rightarrow OH + NO_2 \quad : k_5 \tag{R7}$$

In the urban atmosphere, we can assume that the produced HO_2 and RO_2 radicals react with NO to produce NO_2 because of high level NO_x, and that O_3 is subsequently produced by photolysis of NO_2. Therefore, the production rates of HO_2 and RO_2 ($P_{RO_2HO_2}$) play a substantial role in determining the production rate of O_3. The ozone production potential is proportional to the number of accumulated HO_2 and RO_2 radicals through the radical propagation cycle from a single OH radical. The production rate of RO_2 and HO_2 radicals $P_{RO_2HO_2}$ and ozone production potential Φ are defined as follows.

$$P_{RO_2HO_2} = k_2[CO][OH] + 2\Sigma k_{1i}[VOC_i][OH] \tag{2}$$

$$\Phi = \frac{\int_0^\infty P_{RO_2HO_2}\,dt}{[OH]_0} \tag{3}$$

Here, $[OH]_0$ is the initial OH concentration, which is OH generated by primary sources such as O_3 photolysis. $[OH]_0$ was set to the appropriate concentration (typically 10^6 molecules cm^{-3}). $\Sigma k_{1i}[VOC_i][OH]$ is the summation of reactivity of OH + VOC_i. The VOC_i reactivity was obtained from both observed (combination of missing OH reactivity and known VOCs reactivity) and calculated OH reactivity in this study. Fig. 9 shows the ozone production potential in the summer period. The ozone production potential obtained from directly measured OH reactivity was significantly higher than that obtained from calculated OH reactivity, particularly under lower NO_x conditions (<30 ppbv). This is also similar to the results obtained during autumn, although the ozone production potential was lower than that in summer. When the NO_x concentration is higher than 30 ppbv, the NO_2 + OH reaction is dominant and inhibited O_3 production. On the other hand, under low NO_x conditions, the NO_2 + OH reaction is inhibited while ozone production efficiency is nonlinearly enhanced because VOCs + OH reactions are facilitated. This suggests that the missing OH reactivity owing to unknown VOCs contributed significantly to photochemical ozone production in the urban atmosphere.

4. Conclusion

We conducted comprehensive observations in Toyocho, Koto-ku, Tokyo, in the summer and winter of 2007 and in the autumn of 2009. The observation site was situated in central Tokyo, where there were primary anthropogenic emissions such as vehicle exhaust and emissions from factories. The observed trace species had large variations because the site was close to these emission sources and directly reflected the primary emissions. A large variation in OH reactivity was also observed.

O_3 variations were typical of an urban atmosphere, in that concentrations were high in the daytime and low in the morning and evening. O_3 concentrations higher than 120 ppbv were observed in summer, while in winter and in autumn, O_3 remained at 20–40 ppbv. NO and NO_2 also showed variations that were typical of an urban atmosphere, in that they increased in the morning and in the evening rush hour, and decreased around noon. A comparison of NO and CO indicates that in winter and in autumn, they exhibited a good correlation, while in summer, they did not. These results show that primary vehicle emissions were the dominant NO source in winter and in autumn, while photolysis of NO_2 was significant in summer, along with vehicle emissions.

The total NMHC concentration was higher in winter than in summer and in autumn. This reflects a reduction in the loss processes of NMHCs because of the low OH levels in winter. OVOCs were present in higher concentrations in summer than in winter and autumn. This reflects the importance of the photochemical production of OVOCs.

The level of OH reactivity ranged from 10 to 80 s^{-1} in all periods, with values that were higher than those obtained in Hachioji, a suburban area. OH reactivity was high in the morning and the evening rush hour, which reflects primary emissions from vehicle exhaust. The missing OH reactivity was observed on all days. The missing OH reactivity may be at least partly due to unknown VOC species produced from photochemical reactions in the atmosphere and/or primary emissions sources in the urban environment. The missing OH reactivity significantly contributed to the ozone production potential, particularly under low NO_x conditions during the summer period. With the breakdown of OH reactivity, NO_x accounted for a large contribution to OH reactivity in autumn, while VOCs accounted for a large value in summer, despite showing similar values for total OH reactivity. These results indicate the presence of different dominant processes in atmospheric reactions that are dependent upon the season.

Acknowledgments

We are grateful to our colleagues for support of the observations, and Dr. C. Jones for assistance this work. This work was

financially supported by Ministry of Educations and Science, Sports, and Culture of Japan (Grant-in-Aid No. 21221001). A part of this research has been performed commissioned by Ministry of Economy, Trade, and Industry of Japan, and as part of a collaborative research program between auto and oil industries called Japan Auto-Oil Program (JATOP) run by Japan Petroleum Energy Center.

References

Akimoto, H., 2006. Tropospheric Ozone: A Growing Threat. Publications of Acid Deposition an Oxidant Research Center, Niigata Japan.

Atkinson, R., Baulch, D.L., Cox, R.A., Hampson Jr., R.F., Kerr, J.A., Rossi, M.J., Troe, T., 1997. Evaluated kinetic and photochemical data for atmospheric chemistry: supplement VI. Journal of Physical and Chemical Reference Data 26, 215–290.

Atkinson, R., 1994. Gas-phase tropospheric chemistry of organic compounds. Journal of Physical and Chemical Reference Data, Monograph 2, 1–216.

Atkinson, R., 1997. Gas-phase tropospheric chemistry of volatile organic compounds: 1. Alkanes and alkenes. Journal of Physical and Chemical Reference Data 26, 215–290.

Atkinson, R., 2003. Kinetics of the gas-phase reactions of OH s with alkanes and cycloalkanes. Atmospheric Chemistry and Physics 3, 2233–2307.

Bureau of Environment, Tokyo Metropolitan Government, 2010. Air Pollution Control, The Environment of Tokyo 2010, 84–93 pp. (in Japanese).

Calvert, J.G., Atkinson, R., Kerr, J.A., Madronich, S., Moortgat, G.K., Wallington, T.J., Yarwood, G., 2000. Reaction of alkenes with the OH radical. In: The Mechanisms of Atmosphere Oxidation of Alkenes. Oxford University Press, New York, pp. 23–126.

Chatani, S., Shimo, N., Matsunaga, S., Kajii, Y., Kato, S., Nakashima, Y., Miyazaki, K., Ishii, K., Ueno, H., 2009. Sensitivity analyses of OH missing sinks over Tokyo metropolitan area in the summer of 2007. Atmospheric Chemistry and Physics 9, 8975–8986.

Goldan, P.D., Parrish, D.D., Kuster, W.C., Trainer, M., McKeen, S.A., Holloway, J., Jobson, B.T., Sueper, D.T., Fehsenfeld, F.C., 2000. Airborne measurements of isoprene, CO, and anthropogenic hydrocarbons and their implications. Journal of Geophysical Research 105, 9091–9105.

Goldstein, A.H., Galbally, A.E., 2007. Known and unexplored organic constituents in the earth's atmosphere. Environmental Science and Technology 41, 1514–1521.

Hofzumahaus, A., Roher, F., Lu, K., Bohn, B., Brauers, T., Chang, C.-C., Fuchs, H., Holland, F., Kita, K., Kondo, Y., Li, X., Lou, S., Shao, M., Zeng, L., Wahner, A., Zhang, Y., 2009. Amplified trace gas removal in the troposphere. Science 324, 1702–1704.

Kajii, Y., Yoshino, A., Watanabe, K., Sadanaga, Y., Matsumoto, J., Nishida, S., Kato, S., 2006. Evaluation of oxidant potential in the semi-urban atmosphere. Journal of Japan Society of Atmospheric Environment 41, 259–267 (in Japanese).

Kato, S., Pochanart, P., Kajii, Y., 2001. Measurements of ozone and nonmethane hydrocarbons at Chichijima island, a remote island in western Pacific: long-range transport of polluted air from the Pacific rim region. Atmospheric Environment 35, 6021–6029.

Kato, S., Miyakawa, Y., Kaneko, T., Kajii, Y., 2004. Urban air measurements using PTR-MS in Tokyo area and comparison with GC–FID measurement. International Journal of Mass Spectrometry 253, 103–110.

Lewis, A.C., Carslaw, N., Marriott, P.J., Kinghorn, R.M., Morrison, P., Lee, A.L., Bartle, K.D., Pilling, M.J., 2000. A larger pool of ozone-forming carbon compounds in urban atmospheres. Nature 405, 778–781.

Lou, S., Holland, F., Roher, F., Lu, K., Bohn, B., Brauers, T., Chang, C.C., Fuchs, H., Häseler, R., Kita, K., Kondo, Y., Li, X., Shao, M., Zeng, L., Wahner, A., Zhang, Y., Wang, W., Hofzumahaus, A., 2010. Atmospheric OH reactivities in the Pearl River Delta – China in summer 2006: measurement and model results. Atmospheric Chemistry and Physics 10, 11243–11260.

Mao, J., Ren, X., Chen, S., Brune, W.H., Chen, Z., Martinez, M., Harder, H., Lefer, B., Rappenglück, B., Flynn, J., Leuchner, M., 2010. Atmospheric oxidation capacity in the summer of Houston 2006: comparison with summer measurements in other metropolitan studies. Atmospheric Environment 44, 4107–4115.

Matsumoto, J., Kajii, Y., 2003. Improved analyzer for nitrogen dioxide by laser-induced fluorescence technique. Atmospheric Environment 37, 4847–4851.

Matsumoto, J., Hirokawa, J., Akimoto, H., Kajii, Y., 2001. Direct measurement of NO_2 in the marine atmosphere by laser-induced fluorescence technique. Atmospheric Environment 35, 2803–2814.

Nakashima, Y., Kamei, N., Kobayashi, S., Kajii, Y., 2010. Total OH reactivity and VOC analyses for gasoline vehicular exhaust with a chassis dynamometer. Atmospheric Environment 44, 468–475.

Ohara, T., Sakata, T., 2003. Long-term variation of photochemical oxidants over Japan. Journal of Japan Society for Atmospheric Environment 38, 47–54 (in Japanese).

Ren, X., Harder, H., Martinez, M., Lesher, R.L., Oliger, A., Shirley, T., Adams, J., Simpas, J.B., Brune, W.H., 2003a. HO_x concentrations and OH reactivity observations in New York City during PMTACS-NY2001. Atmospheric Environment 37, 3627–3637.

Ren, X., Harder, H., Martinez, M., Lesher, R.L., Oliger, A., Simpas, J.B., Brune, W.H., Schwab, J.J., Demerjian, K.L., He, Y., Zhou, X., Gao, H., 2003b. OH and HO_2 chemistry in the urban atmosphere of New York City. Atmospheric Environment 37, 3639–3651.

Ren, X., Brune, W.H., Mao, J., Mitchell, M.J., Lesher, R.L., Simpas, J.B., Metcalf, A.R., Schwab, J.J., Cai, C., Li, Y., Demerjian, K.L., Felton, H.D., Boynton, G., Adams, A., Perry, J., He, Y., Zhou, X., Hou, J., 2006. Behavior of OH and HO_2 in the winter atmosphere in New York City. Atmospheric Environment 40, S252–S263.

Sadanaga, Y., Yoshino, A., Yoshioka, A., Watanabe, K., Kato, S., Matsumoto, J., Wakazono, Y., Kanaya, Y., Kajii, Y., 2004a. Development of a measurement system of OH reactivity in the atmosphere by using a laser-induced pump and probe technique. Review of Scientific Instruments 75 (8), 2648–2655.

Sadanaga, Y., Yoshino, A., Kato, S., Yoshioka, A., Watanabe, K., Miyakawa, Y., Hayashi, I., Ichikawa, M., Matsumoto, J., Nishiyama, A., Akiyama, N., Kajii, Y., 2004b. The importance of NO_2 and volatile organic compounds in the urban air from the viewpoint of the OH reactivity. Geophysical Research Letters 31, L08102. doi:10.1029/2004GL019661.

Sadanaga, Y., Yoshino, A., Kato, S., Kajii, Y., 2005. Measurements of OH reactivity and photochemical ozone production in the urban atmosphere. Environmental Science and Technology 39, 8847–8852.

Sadanaga, Y., Kondo, S., Hashimoto, K., Kajii, Y., 2006. Measurement of the rate coefficient for the OH + NO_2 reaction under the atmospheric pressure: its humidity dependence. Chemical Physics Letters 419, 474–478.

Sander, S.P., Friedl, R.R., DeMore, W.B., Golden, D.M., Kurlyo, M.J., Huie, R.E., Orkin, V.L., Moortgat, G.K., Ravishankara, A.R., Kolb, C.E., Molina, M.J., Finlayson-Pitts, B.J., 2002. Chemical Kinetics and Photochemical Data for Use in Atmospheric Studies Evaluation Number 14. JPL Publication 02-25.

Sharma, U.K., Kajii, Y., Akimoto, H., 2000. Characterization of NMHCs in downtown urban center Kathmandu and rural site Nagarkot in Nepal. Atmospheric Environment 34, 3297–3307.

Shirley, T.R., Brune, W.H., Ren, X., Mao, J., Lesher, R., Cardenas, B., Volkamer, R., Molina, L.T., Molina, M.J., Lamb, B., Velasco, E., Jobson, T., Alexander, M., 2006. Atmospheric oxidation in the Mexico City metropolitan area (MCMA) during April 2003. Atmospheric Chemistry and Physics 6, 2753–2765.

Sinha, V., Williams, J., Crowley, J.N., Lelieveld, J., 2008. The comparative reactivity method: a new tool to measure total OH reactivity in ambient air. Atmospheric Chemistry and Physics 8, 2213–2227.

Tajima, Y., Kato, S., Suthawaree, J., Kajii, Y., 2010. Long-term measurement of various volatile organic compounds and air quality assessment using OH reactivity and ozone formation potential in sub-urban area of Tokyo. Journal of Japan Society of Atmospheric Environment 45, 56–64 (in Japanese).

Yoshino, A., Sadanaga, Y., Watanabe, K., Kato, S., Miyakawa, Y., Matsumoto, J., Kajii, Y., 2006. Measurement of total OH reactivity by laser-induced pump and probe technique – comprehensive observations in the urban atmosphere of Tokyo. Atmospheric Environment 40, 7869–7881.